Science Arts & Métiers (SAM)

is an open access repository that collects the work of Arts et Métiers Institute of Technology researchers and makes it freely available over the web where possible.

To cite this version :

Off-line path programming for three-dimensional Robotic Friction Stir Welding based on Bézier curves

Komlan Kolegain[a]; François Léonard[b]; Sandra Chevret[b]; Amarilys Ben Attar[a]; Gabriel Abba[b]

[a] *Institut de soudure, Goin, France*
[b] *Design, Manufacturing and Control Laboratory, Arts et Metiers ParisTech, Universite de Lorraine, Metz, France*

Abstract

Purpose - Robotic Friction Stir Welding (RFSW) is an innovative process which enables solid-state welding of aluminum parts with robots. A major drawback of this process is that the robots joints undergo elastic deformations during the welding due to the high forces induced by the process. This leads to the tool deviation and wrong orientation. Today, there is no CAM/CAD software to generate off-line paths which integrates robot deflections. The main objective of this work is to propose an off-line methodology to plan path for robotic friction stir welding.

Design/methodology/approach - The approach is subdivided in two stages. The first stage consists on extracting position and orientation data from CAD models of the workpieces and adding it the deflections calculated with a deflection model in order to have a suitable path for performing RFSW. The second stage consists on fitting the suitable path in a smooth path using Bézier curves.

Findings - The method is experimented and validated by performing a welding on a curve workpiece with a robot Kuka KR500-2MT. A suitable tool position and orientation were calculated to perform this welding, an experimental procedure was set up, free defect weld was performed and high accuracy in position and orientation was achieved.

Practical implications - The method will help manufacturers to perform easily RFSW for 3D workpieces regardless the lateral tool deviation, lost of the right orientation and control force stability.

Originality/value - The originality of the method is to compensate robot deflections without using expensive sensors which is the most used method for robot deflection compensation. This off-line method can leads to reduce programming time in comparison with teach programming method and leads to reduce investments costs in comparison with the commercial off-line programming packages.

Keywords Robotic friction stir welding, deflection model, path planning, off-line programming, Bézier curves.

Paper type Research paper

1 Introduction

The Friction Stir Welding (FSW) process consists in a tool composed by a pin and a shoulder put in rotation and plunged between two clamped parts. Then the tool is moving along the weld line with the shoulder in contact with the workpiece surface. Therefore, FSW requires applying a high down-force on the workpiece. FSW as a solid state welding process allows the welding of all the aluminum alloys keeping good mechanical properties in particular in fatigue resistance as demonstrated by (Zhou et al., 2005). The FSW process presents real interest in aerospace and automotive industries (Lyles et al., 2016), (Kusuda, 2013). The machines commonly used industrially are dedicated ones (see (Okawa et al., 2006)) which require high investment costs. To reduce the investments costs, robots can be used as FSW machine. (Cook et al., 2004), (Soron and Kalaykov, 2006), (Voellner et al., 2006), (Zaeh and Voellner, 2010) used serial manipulator robot with a force feedback control technique to perform 2D and 3D FSW. A review of machines and control system for FSW can be found in (Mendes et al., 2016). Serial industrial robots have lower investment cost and allow the welding of complex geometries but they undergo deflection under the load applied during the welding leading the tool to deviate in the transverse or lateral direction (Voellner et al., 2007),(De Backer et al., 2010). To perform FSW, (Zimmer et al., 2008) illustrated the ideal tool position and orientation during welding (see Fig.1). The tool has to be placed according to the workpiece surface. At each point of

the seam, the tool coordinate system has to be tilted in the welding direction with a certain angle, commonly with a 1° to 3° angle according to the normal vector to the surface (see Fig.1). Under high loads, the tilt angle must be maintained in a nominal interval during the welding operation. Otherwise, the weld could present defects as described by (Zimmer-Chevret et al., 2014), (Shultz et al., 2010), (Chen et al., 2006).

So, the tool path (position and orientation) must be well planned to succeed robotic FSW (RFSW) of 3-dimensional weld geometries. There are different techniques to plan the robot path (Pan et al., 2012). The classical technique is the online programming where points are taught with a teach pendant. This technique requires more time for complex paths programming and the presence of the operator near to the robot. Also, the points have to be re-taught when the task changes. To overcome this drawback, commercials softwares packages such as Delmia© (Polden et al., 2011), RobCad© (Dong et al., 2007), RobotMaster©, RobotStudio©, KUKA.Sim© were proposed to program off-line the robot path. This consists on generating automatically the robot's tool path from the CAD drawing of the workpieces. Apart from their high costs, the limit of these off-line packages to plan path for RFSW is that it doesn't take into account the tool deviation due to the high forces induced by the process. It is so necessary to develop an off-line specific method to plan path for RFSW like those developed by researchers for different applications such as deburring of aerospace components (Leali et al., 2013), spray painting (Andulkar et al., 2015), arc welding (Chen et al., 2015) and laser cladding (Zheng et al., 2016). The techniques can be used to generate the robot path from CAD drawings are parametric curves such as splines, Bézier curves, B-splines or Non-Uniform Rational Basis Spline (NURBS). (Jahanpour et al., 2016) used NURBS method to generate path from CAD drawing for a machining application; (Neubauer and Müller, 2015) used B-splines for a polishing application; (Giberti et al., 2017) used Bézier curves to plan path for robotic additive manufacturing. For the FSW process, (Soron and Kalaykov, 2007) used cubic parametric curve to generate the tool path. Their method is based on extracting topological entities in the CAD drawing from which they defined the path segments modeled by cubic polynomials. The limit of their method is that they don't take into account the deflections of the robot in the path planning likewise the off-line commercial software packages used to plan path for FSW.

In this paper, we proposed to use the Bézier curve technique to generate off-line optimized tool path that take into account the robot deflections from CAD drawings. Having G^∞ continuity, the Bézier curves presents the advantage to generate smooth path. Despite the fact that Bézier curves can't approximate rigorously an arc of circle, the precision obtained in our application, allow us to use the Bézier curve instead of using the B-splines or NURBS which are the generalization of the Bézier curves. For other complex paths, B-splines or NURBS can be investigated. Due to the tool deviation and disoriented caused by the compliance of the robot, the compensation of the robot deflection is taken into account in the path planning. There are two techniques to compensate robot deflection: online compensation and off-line compensation. The online compensation technique is based on feedback control and the compensation is done in real time (Qin et al., 2016), (Guillo and Dubourg, 2016), (De Backer and Bolmsj, 2014), (De Backer et al., 2012). In this paper, to generate automatically the robot path from CAD models, an off-line compensation technique is choosed. This technique was used by (Belchior et al., 2013) to compensate tool path deviations on robotic sheet forming. Similar to this technique, we propose to calculate along the desired welding path all deflections of the robot by using a deflection model identified in (Qin, 2013). These deflections are then added to the desired welding path extracted form CAD drawings in order to have a suitable path for RFSW. Then a smooth path is generating from the suitable path by using the Bézier curve technique.

By applying the proposed approach on welding experiments of a curvilinear path, high accuracy path was achieved, less tool lateral deviation was measured and free-defect weld was performed.

The paper is organized as follow. In section 2, the deflection model of an industrial robot manipulator is presented. In the section 3, the methodology to plan a FSW path using Bézier
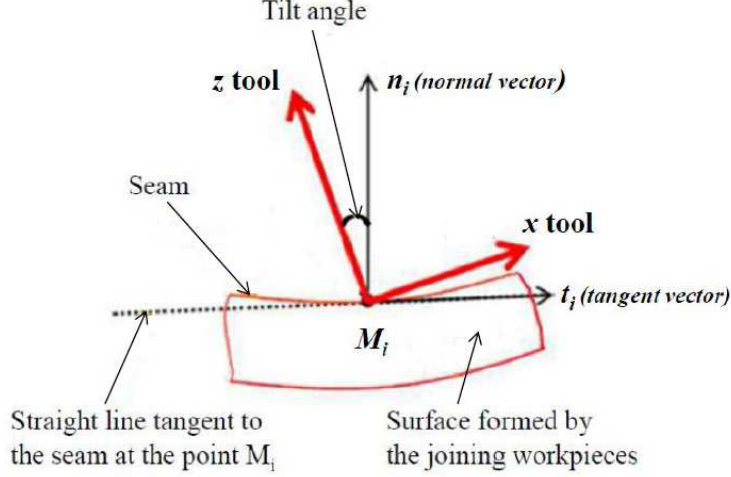
Figure 1: Theoretical tool orientation along the welding path

curves is detailed. In section 4, the welding experiments are presented and the results are discussed. The conclusions and future works are presented in section 5.

2 Robot modeling

The robot used during the welding experiments is a KUKA KR 500-2MT industrial heavy load robot. To define the task in the robot frame, we need two types of models: the kinematic models and the deflection model.

2.1 Kinematic models

The kinematic models define the relation between the joints coordinates and the pose (position and orientation) of the tool and inversely. The Denavit-Hartenberg parameters of the six joints are defined precisely in (Qin, 2013) and (Qin et al., 2014). The detailed expressions of the forward and inverse kinematics are given in (Qin, 2013). The numerical values of the links length are expressed in appendix.

2.2 Deflection model

The deflection model describes the relation between the tool end pose under load and without load. Under FSW load, the robot applies a wrench W of forces and torques on the external environment. This wrench is expressed as:

$$W = [F_x\, F_y\, F_z\, T_x\, T_y\, T_z]^\top \tag{1}$$

where F_x, F_y and F_z are the forces acting by the FSW tool on the workpiece; the torques T_x and T_y are negligible and the torque T_z is due to the rotation of the spindle.

Under the assertion that the deformation of the robot is mainly located on the joint axes (Dumas, 2011), we define the model of torsional deformation given in Fig. 2. This model supposes that all deformations can be located on the output of the gearboxes. The identification method of (Jubien et al., 2014) is used to determine the numerical value of the coefficients of the stiffness matrix K. During the identification, the robot bodies support bending constraints. The corresponding deflection is also integrated in the stiffness matrix.

The relation between the gearbox output torque vector Γ and the joint angle variation is given by:

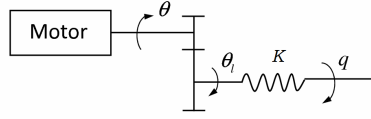$$\Gamma = K(N^{-1}\theta - q) = K\Delta q \tag{2}$$

3

Figure 2: Torsional deformation model of a gearbox

where $q = [q_1 \, q_2 \, q_3 \, q_4 \, q_5 \, q_6]^\top$ is vector of angular positions of the joint, $\theta_l = N^{-1}\theta$ is the angular position after gear reduction and Δq is the angular deformation of the gearbox output. The gear ratio matrix N is a matrix of dimension 6×6. For the robot KUKA KR500-2MT, N is not a diagonal matrix because of the coupling among axes 4, 5 and 6. The non-null elements of matrix N and K are presented in appendix.

A general form of the robot's dynamic model can be expressed as:

$$\Gamma = D(q)\ddot{q} + H(q, \dot{q}) + F_f(\dot{q}) + J^\top(q)W \qquad (3)$$

where $D(q)$ is the symmetric, uniformly positive defined and bounded inertia matrix of the robot and $H(q, \dot{q})$ represents the contribution due to centrifugal, Coriolis and gravitational forces and the gas jack of axis two, $F_f(\dot{q})$ is the vector of friction torque applied on the joints, $J^\top(q)$ is the Jacobian matrix and vectors $\dot{q}$ and $\ddot{q}$ represent angular velocities and accelerations.

During FSW tasks, the cartesian speed and acceleration of the tool are relatively low. So we can neglect the inertia, centrifugal, Coriolis and friction terms and the equation (3) is reduced to:

$$\Gamma = J^\top(q)W + H(q, 0) \qquad (4)$$

where $H(q, 0)$ represents the gravitational forces vector. The cartesian deformation of the robot and the roll, pitch and yaw angles variations are obtained by:

$$\begin{bmatrix} \Delta P \\ \Delta \Theta \end{bmatrix} = L_a \, J(q) \, \Delta q \qquad (5)$$

where $\Delta P = [\Delta X \, \Delta Y \, \Delta Z]^\top$ is the cartesian displacement of the tool end under external wrench, $\Delta \Theta = [\Delta A \, \Delta B \, \Delta C]^\top$ is the corresponding angular variation of the orientation angles and L_a is a matrix defined in the appendix.

We suppose here that the wrench W is known. The deflections along a welding path can be calculated off-line by the formula below:

$$\begin{bmatrix} \Delta P \\ \Delta \Theta \end{bmatrix} = L_a \, J(q) \, K^{-1} \left(J^\top(q) \, W + H(q, 0) \right) \qquad (6)$$

3 Path planning methodology

The proposed methodology consists on extracting geometrical information from a CAD model, estimating the deflections and generating the FSW path by using the Bézier curve technique.

3.1 Extraction of data from CAD models

The position of a FSW tool is represented by three components (x, y, z) and the orientation can be represented by the angles of yaw-pitch-roll. In the Kuka robot controller, these angles are noted A, B and C. To extract data from CAD model, different methods can be used. (Zheng et al., 2016) and (Soron and Kalaykov, 2007) developed algorithms to extract topological information such as lines and arcs from the CAD model while (Neto and Mendes, 2013)

developed algorithms to extract both positional and orientation data from CAD drawing by using Autodesk Inventor© software. In our work, a method which can be used with any CAD software is choosed. By setting a frame (O, x, y, z) in the CAD environment, the three position coordinates (x, y, z) of n points coming from the discretization of the path can be retrieved and the orientation coordinates can be calculated.

3.2   Approximation of a path by Bézier curve

Bézier curves are polynomial parametric curves which can be used to model complex paths. An nth-order Bézier curve $P(u)$ is defined by:

$$P(u) = \sum_{i=0}^{n} P_i \frac{n!}{i!(n-i)!} u^i (1-u)^{n-i} \tag{7}$$

where u is a normalized parameter and $P_i \in \mathbb{R}^n$ are the control points.

The geometrical coordinates extracted from a CAD model can be approximated by a Bézier function. Consider $X = [x_0 \cdots x_m]^\top$ and $Z = [z_0 \cdots z_m]^\top$, two vectors obtained from the x and z coordinates extracted from the CAD model. Defined for all $i \in [0 \cdots m]$:

$$u_i = \frac{x_i - x_0}{x_m - x_0} \tag{8}$$

and

$$Z_b(u_i) = \sum_{i=0}^{n} P_{iz} B_i^n(u_i) \tag{9}$$

where $B_i^n(u) = \frac{n!}{i!(n-i)!} u^i (1-u)^{n-i}$. Then, the control points P_{iz} are obtained by solving a minimization problem defined by $\min \| Z - Z_b \|$. For $m \gg n$, the least squares method can be used to obtain:

$$P_z = [P_{0z} \cdots P_{nz}]^\top = \left(M^\top M\right)^{-1} M^\top Z \tag{10}$$

where $M = \begin{bmatrix} B_0^n(u_0) & \cdots & B_n^n(u_0) \\ \vdots & \ddots & \vdots \\ B_0^n(u_m) & \cdots & B_n^n(u_m) \end{bmatrix}$

Once the coefficients P_z are determined, the Bézier function Z_b which approximate the z coordinate of the path can be computed. Afterwards, the maximum error due to the approximation can be calculated by the relation:

$$e_z = \max_{i \in [1,m]} \left(Z_b(u_i) - Z(u_i)\right) \tag{11}$$

If the maximum error is too high for an nth order Bézier function, one can increase the order to $n+1$ until the error is lower as a defined constant ξ.

The method used for the z coordinate can be extended to obtain the Bézier functions for all coordinates.

3.3   Methodology for approximating a FSW path

The goal of the research work is to propose a methodology to program off-line a 3-dimensional FSW path which take into account the robot deformation. It consists on generating an optimized path P_{BP} which includes the path extracted from the CAD model and the deflection along the path.
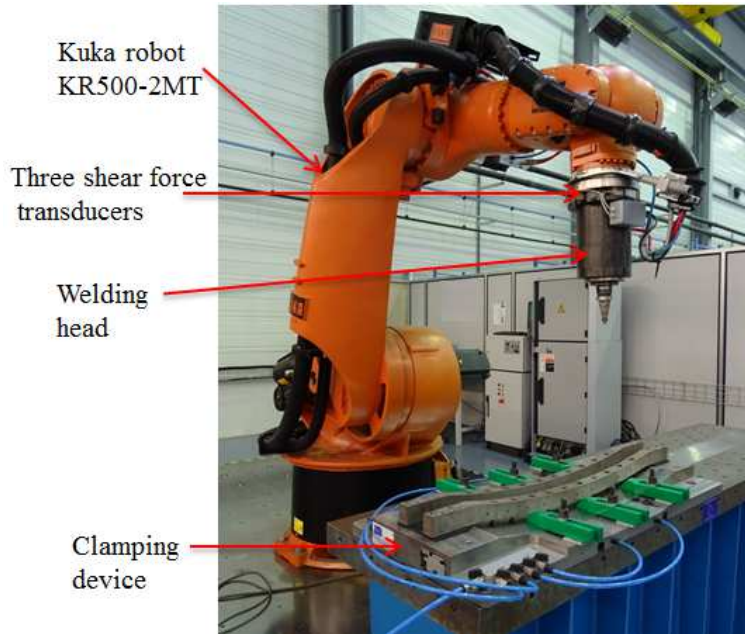
$$P_{BP} = P_{CAD} + \Delta P \tag{12}$$

Figure 3: RFSW experimental setup

where P_{BP} is the optimized path, P_{CAD} is the path extracted from the CAD model, ΔP is determined by the deflection model (see Eq.6).

Finally, to approximate a FSW path by Bézier curves, two steps are needed. The first step is to extract nominal data from the CAD model of the workpiece and to add the robot deflection calculated on the same position. The second one is the fitting of these data P_{BP} by using the Bézier curves technique previously described. This methodology have to be validated by performing experiments.
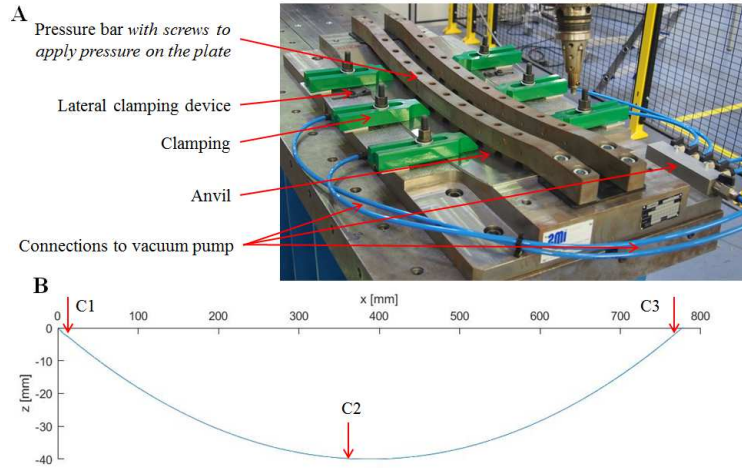
4 Experiments

4.1 Experimental setup

All the experiments were performed on a FSW robot used for developing industrial applications. The robot KUKA KR 500-2MT is equipped with a welding head (see Fig.3). Between the welding head and the 6th robot axis, three shear force transducers are arranged in tilt position by 120° each around the longitudinal axis. It permits to calculate precisely the downforce applied on the tool during welding.

Note that in our experiments, any joining operation isn't performed. The validation of the methodology consists on performing the path generated off-line on a test workpiece. The test workpiece, a 2 mm thick aluminum alloy EN AW-2024 T3, is placed inside the clamping device such that on all the length, the back of the plate perfectly fit on the clamping device, Fig.4-A. To achieve this, next to the welding zone, the clamping device possesses a vacuum field permitting to ensure a proper fit-up between the workpiece and the anvil. Table 1 shows the welding conditions during the experiments. The tool tilt angle is 2.5°. The robot is controlled in force in z tool direction (desired value 8000 N) and a welding in x world negative direction with an advance speed v_a is programmed. The forces induced in the transverse direction(F_y) and advance direction (F_x) are respectively 150N and 420 N. The torque in the axial direction (T_z) is 75 Nm.

Table 1: Welding experiments conditions

Parameters	Name/Value
Material	EN AW-2024 T3
Thickness (d_m)	2 mm
Advance speed (v_a)	300 mm/min
Rotation speed (Ω)	800 rpm
Tilt angle (α)	2.5°
Axial force (F_z)	8000 N

Figure 4: A: Clamping device; B: Curvilinear path

4.2 Experiments, results and discussions

Considering the CAD model of the test workpiece in which we define a single curvature path (Fig.4). From the CAD model, a discretization of the desired welding path is done. In the robot world coordinate system, the position coordinates (x, y, z) of 100 points are extracted. The 100 points are equidistant and distributed along the desired welding path. The yaw angle A is fixed at 0°. Due to the single0 curvature of the defined path, the roll angle C is fixed constant at 180°. The pitch angle coordinate B for the 100 points are calculated.

Using the deflection model described in the section 2, the deflections ΔY, ΔZ and ΔB for each extracted point are estimated (Fig.5). We remark that the deflections in the y direction and z direction decrease from the beginning of the path to the end. The deflection in y world direction decreases from -2.72mm to -2.20mm and the deflection in z world direction, from -7.24mm to -4.70mm .The estimated deflection in pitch angle B is quasi-constant and equals to $-0.23°$. The deflection calculated in y world direction represents the tool's lateral deviation. It will be used to correct the tool position in the welding transverse direction. The deflection calculated in z world direction is used to help the force controller to calculate less correction in z tool direction and therefore, maintain easily the downforce at the desired value. For this case of study, the deflection calculated in pitch angle B is too small to influence the orientation of the tool. It can be neglected in the generation of the path. Contrary to the deflection in pitch angle B, the estimated deflections in y world direction and z world direction were added to the coordinates y and z extracted from the CAD model in order to have an optimized tool path which will be approximated by Bézier curves.

We want to achieve an approximating precision under $\xi = 0.01$ mm in y and z coordinate which is sufficient to perform a FSW experiment. A 3rd order Bézier function doesn't permit to obtain the fixed precision. So, we increase the order to compute a 5th order Bézier function.
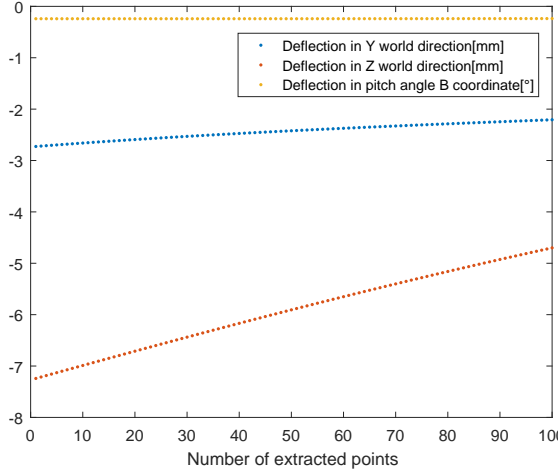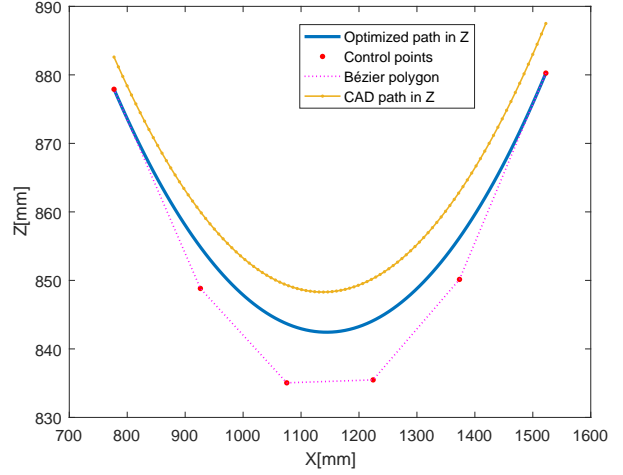
Figure 5: Estimated deflections

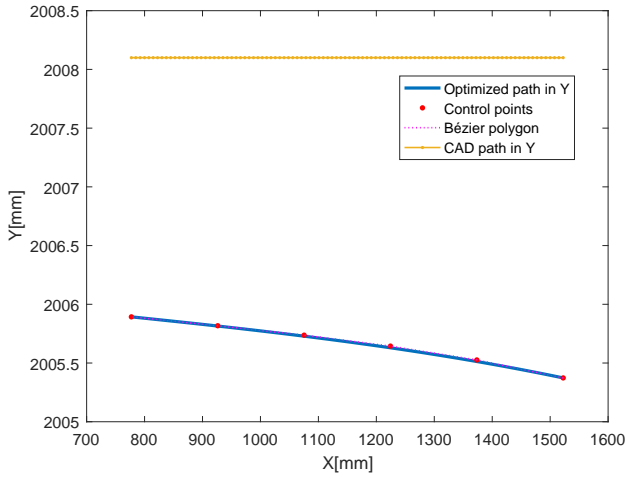**Figure 6:** Tool path in robot world z direction

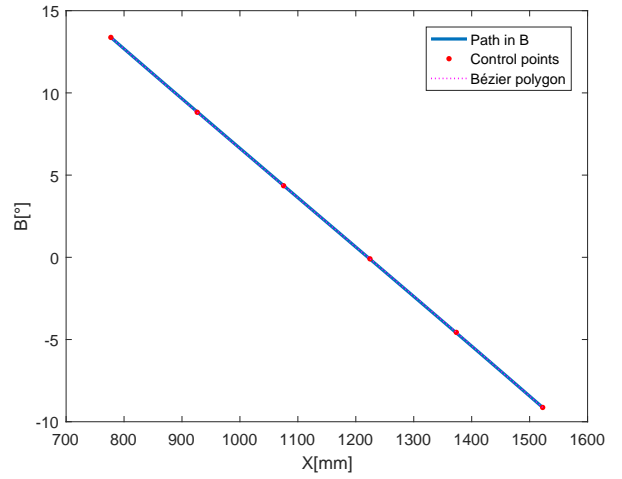**Figure 7:** Tool path in robot world y direction

Figure 8: Tool path in pitch angle B

The 5th order Bézier function was also computed for the pitch angle B coordinate. The different coefficients of control points for Bézier curves can been found in Table 2. Figures 6, 7 show respectively the optimized tool path approximated by Bézier curves in z, y coordinates. By neglecting the deflection calculated in pitch angle B, the optimized path in B coordinate is the same as the pitch angle extracted from the CAD model. The figure 8 shows the CAD tool path in B coordinate approximated by Bézier curves. The smooth path in pitch angle varies from $-9.13°$ at the beginning of the path to $13.77°$ at the end.

Table 2: Coefficients of Bézier curves

Control points	P_0	P_1	P_2	P_3	P_4	P_5
P_x data [mm]	1522,50	1373,446	1224,392	1075,338	926,284	777,229
P_y data [mm]	2005,373	2005,526	2005,643	2005,737	2005,817	2005,893
P_z data [mm]	880,257	850,144	835,477	835,048	848,825	877,899
P_B data [°]	-9,130	-4,564	-0,092	4,353	8,820	13,374

From an experimental point of view, the proposed methodology is based on a dialog between the robot and an external computer by using the technology package Robot Sensor Interface
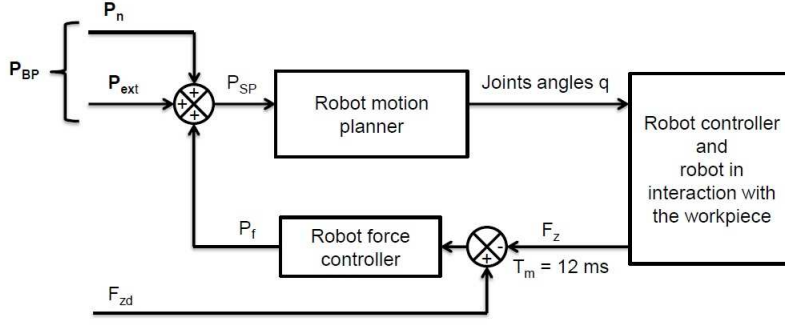
Figure 9: Schematic view of the proposed experimental procedure

(RSI) of the Kuka robot. With the RSI functions, an external computer receives each $T_m = 12$ ms the positions provided by the robot controller and sends back the necessary correction in order to achieve the optimized path planned by Bézier curves. So, the planned Bézier path P_{BP} is decomposed in two paths P_n and P_{ext}. P_n is a nominal path defined in the robot main source program. P_{ext} is a path defined on an external computer. P_{ext} is calculated each $T_m = 12$ ms by a C++ program. On the Kuka controller, the effective path is $P_{SP} = P_{BP} + P_f$ (see Fig.9) where P_f is a input correction provided by the force controller which is only acting in z tool frame direction.

For our test workpiece, the nominal path P_n programmed in the Kuka controller is a line passing through the point C_1 and point C_3 (see Fig.4-B). The external correction path $P_{ext}(k) = [0 \ P_y(k) \ P_z(k) \ 0 \ P_B(k) \ 0]^\top$ calculated each $T_m = 12$ ms is then used during the experiment to adapted the z position, y position and the pitch angle B of the tool with respect to the effective x position of the tool. This experiment is called 'Bézier experiment'. In order to emphasize the results obtained with the 'Bézier experiment', a second experiment called 'robotmaster experiment' is performed. It consists on generating the tool path with the commercial software package RobotMaster©.

In order to measure the lateral deviation with a microscope, a reference tool path corresponding to the desired P_{CAD} path was drawn in the welding seam. The lateral deviation equals to the difference between the distance from the reference path to the border of the welding seam (r_m) and the radius of the tool shoulder (r_s=5mm) (see fig.10). The figure 11 shows the lateral tool deviation measured along the welding seam. For the Bézier experiment, the tool deviation varies from 0.42mm at the beginning of the path to 0.2mm at the end. At the middle of the path, it equals to 0.02mm. The RMS value of the tool deviation measured is 0.24mm for the Bézier experiment whereas it equals to 2.8mm for the robotmaster experiment. Our proposed methodology permits to reduce significantly the tool deviation. The residual tool deviation measured along the seam is linked to the deflection model used during the experiment. It can strive towards null by taking into account more parameters such as the friction forces in the deflection model.
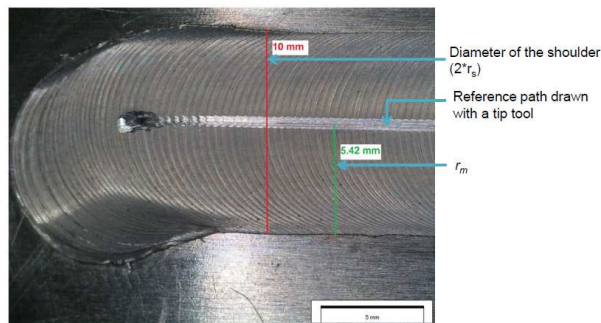

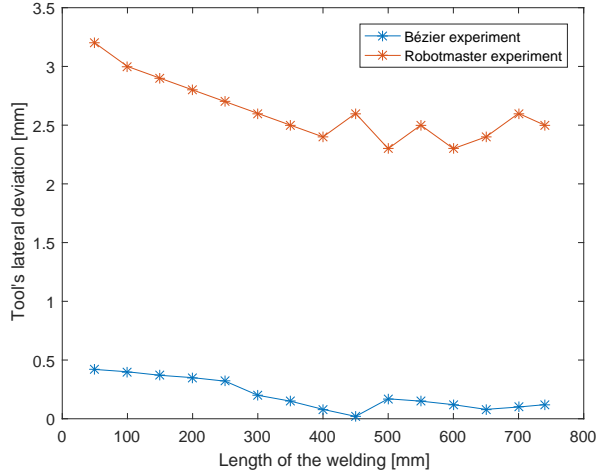**Figure 10:** Measuring principle of tool deviation

9

Figure 11: Tool lateral deviation

Figure 12 represents the measured force F_z. The dive phase consists of three setpoint levels of force of 600 N, 2000 N and 8000 N. We can notice that the mean value of the downforce force F_z remains constant during the experiment contrary to the disturbance in force observed during Robotmaster experiment (Fig.13). In fact, the Kuka force controller does not succeed in maintaining the desired value of 8000 N towards the end of the welding. This is explained by the non compensation of the robot deformation in z direction by using RobotMaster$^{\copyright}$ to generate the path.
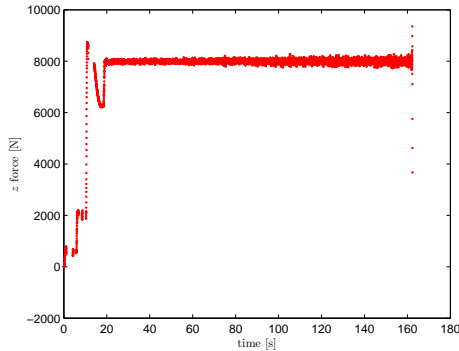

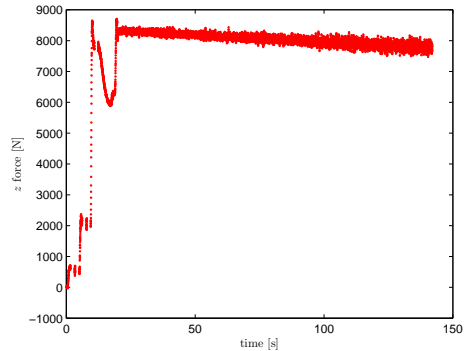**Figure 12:** Axial force F_z during Bézier experiment

Figure 13: Axial force F_z during robotmaster experiment

Neither the visual analysis of the welding seam obtained during the Bézier experiment revealed any surface defects; nor the macrographic analysis revealed any internal defects originated by a wrong orientation of the tool. It implies that free defect welding was performed and the robot succeeds to maintain the correct tool orientation. It validates also the hypothesis of neglecting the deflection in pitch angle B for our test workpiece.

5   Conclusion and future works

In this paper, a path planning methodology based on Bézier curves is presented to perform RFSW. Theoretical and experimental procedures of the methodology were presented. The methodology experimented on a single curvature path permits to obtain a good accuracy in position and orientation. With this methodology, the rms error in the lateral direction has been reduced significantly from 2.8mm to 0.24mm. This precision obtained is very interesting for the welding of aircraft parts which require high precision. The method permits also to help the force controller maintaining easily the downforce at the desired value which is a necessary condition to validate a friction stir welding operation.

The method presents an effective solution to program more simply and more accurately any 3D robotic friction stir welding path. Future works will be interested in validating the methodology for the welding of double curvature aircraft parts like fuselage where the yaw, pitch and roll angles varies simultaneously leading to the control of both the process tilt angle and side-tilt angle. Also, the robot deflection model parameters will be identified with more precision in order to achieve a very high accuracy path programming in position and orientation.

References

Andulkar, M., Chiddarwar, S. and Marathe, A. (2015), 'Novel integrated offline trajectory generation approach for robot assisted spray painting operation', *Journal of Manufacturing Systems* **37**, 201–216.

Belchior, J., Guillo, M., Courteille, E., Maurine, P., Leotoing, L. and Guines, D. (2013), 'Off-line compensation of the tool path deviations on robotic machining: Application to incremental sheet forming', *Robotics and Computer-Integrated Manufacturing* **29**(4), 58–69.

Chen, H.-B., Lin, T. and Chen, S.-B. (2015), 'The application of robotic welding in the shipbuilding', *Advances in Intelligent Systems and Computing* **363**, 483–492.

Chen, H.-B., Yan, K., Lin, T., Chen, S.-B., Jiang, C.-Y. and Zhao, Y. (2006), 'The investigation of typical welding defects for 5456 aluminum alloy friction stir welds', *Materials Science and Engineering A* **433**(1-2), 64–69.

Cook, G., Crawford, R., Clark, D. and Strauss, A. (2004), 'Robotic friction stir welding', *Industrial Robot* **31**(1), 55–63.

De Backer, J. and Bolmsj, G. (2014), 'Deflection model for robotic friction stir welding', *Industrial Robot: An International Journal* **41**(4), 365–372.

De Backer, J., Christiansson, A.-K., Oqueka, J. and Bolmsj, G. (2012), 'Investigation of path compensation methods for robotic friction stir welding', *Industrial Robot* **39**(6), 601–608.

De Backer, J., Soron, M., IIal, T. and Christiansson, A. (2010), Friction stir welding with robot for light weight vehicle design., *in* 'Proc. of 8th International Friction Stir Welding Symposium,Timmendorfer Strand, Germany', pp. 14–24.

Dong, W., Li, H. and Teng, X. (2007), Off-line programming of spot-weld robot for car-body in white based on robcad, *in* '2007 International Conference on Mechatronics and Automation', IEEE, pp. 763–768.

Dumas, C. (2011), Développement de méthodes robotisées pour le parachèvement de pièces métalliques et composites, Phd thesis, in french, Nantes University, Nantes, France.

Giberti, H., Sbaglia, L. and Urgo, M. (2017), 'A path planning algorithm for industrial processes under velocity constraints with an application to additive manufacturing', *Journal of Manufacturing Systems* **43**, 160–167.

Guillo, M. and Dubourg, L. (2016), 'Impact & improvement of tool deviation in friction stir welding: Weld quality & real-time compensation on an industrial robot', *Robotics and Computer-Integrated Manufacturing* **39**, 22–31.

Jahanpour, J., Motallebi, M. and Porghoveh, M. (2016), 'A novel trajectory planning scheme for parallel machining robots enhanced with nurbs curves', *Journal of Intelligent and Robotic Systems: Theory and Applications* **82**(2), 257–275.

Jubien, A., Abba, G. and Gautier, M. (2014), Joint stiffness identification of a heavy kuka robot with a low-cost clamped end-effector procedure, *in* 'Proceedings of the 11th International Conference on Informatics in Control, Automation and Robotics, ICINCO 2014', Vol. 2, Vienna, Austria, pp. 585–591.

Kusuda, Y. (2013), 'Honda develops robotized fsw technology to weld steel and aluminum and applied it to a mass-production vehicle', *Industrial Robot* **40**(3), 208–212.

Leali, F., Pellicciari, M., Pini, F., Berselli, G. and Vergnano, A. (2013), 'An offline programming method for the robotic deburring of aerospace components', *Communications in Computer and Information Science* **371**, 1–13.

Lyles, G., Honeycutt, J. and Cook, J. (2016), Status of nasa's space launch system, *in* '67th International Astronautical Congress, Sept. 26-30, 2016, Guadalajara, Mexico'.

Mendes, N., Neto, P., Loureiro, A. and Moreira, A. (2016), 'Machines and control systems for friction stir welding: A review', *Materials and Design* **90**, 256–265.

Neto, P. and Mendes, N. (2013), 'Direct off-line robot programming via a common CAD package', *Robotics and Autonomous Systems* **61**(8), 896–910.

Neubauer, M. and Müller, A. (2015), Smooth orientation path planning with quaternions using B-splines, *in* 'IEEE/RSJ International Conference on Intelligent Robots and Systems (IROS)', IEEE, pp. 2087–2092.

Okawa, Y., Taniguchi, M., Sugii, H. and Marutani, Y. (2006), Development of 5-axis friction stir welding system, *in* '2006 SICE-ICASE International Joint Conference', pp. 1266–1269.

Pan, Z., Polden, J., Larkin, N., Van Duin, S. and Norrish, J. (2012), 'Recent progress on programming methods for industrial robots', *Robotics and Computer-Integrated Manufacturing* **28**(2), 87–94.

Polden, J., Pan, Z., Larkin, N., Duin, S. and Norrish, J. (2011), 'Offline programming for a complex welding system using DELMIA automation', *Robotic Welding, Intelligence and Automation* pp. 341–349.

Qin, J. (2013), Robust Hybrid Position/Force Control of a Manipulator Used in Machining and in Friction Stir Welding(FSW), Phd thesis, in french, ENSAM, Metz, France.

Qin, J., Léonard, F. and Abba, G. (2014), Nonlinear discrete observer for flexibility compensation of industrial manipulators, *in* 'The 19th IFAC World Congress', Vol. 19, Cap Town, South Africa, pp. 5598–5604.

Qin, J., Léonard, F. and Abba, G. (2016), 'Real-time trajectory compensation in robotic friction stir welding using state estimators', *IEEE Transactions on Control Systems Technology* **24**(6), 2207–2214.

Shultz, E., Cole, E., Smith, C., Zinn, M., Ferrier, N. and Pfefferkorn, F. (2010), 'Effect of compliance and travel angle on friction stir welding with gaps', *Journal of Manufacturing Science and Engineering, Transactions of the ASME* **132**(4), 0410101–0410109.

Soron, M. and Kalaykov, I. (2006), A robot prototype for friction stir welding, *in* '2006 IEEE Conference on Robotics, Automation and Mechatronics', IEEE, pp. 1–5.

Soron, M. and Kalaykov, I. (2007), Generation of continuous tool paths based on CAD models for friction stir welding in 3d, *in* '2007 Mediterranean Conference on Control and Automation, MED'.

Voellner, G., Zaeh, M., Kellenberger, O., Lohwasser, D. and Silvanus, J. (2006), 3-dimensional friction stir welding using a modified high payload robot, *in* '6th International Friction Stir Welding Symposium, Saint Sauveur, Canada', pp. 10–13.

Voellner, G., Zaeh, M., Silvanus, J. and Kellenberger, O. (2007), 'Robotic friction stir welding', *SAE Technical Papers* .

Zaeh, M. and Voellner, G. (2010), 'Three-dimensional friction stir welding using a high payload industrial robot', *Production Engineering* **4**(2), 127–133.

Zheng, H., Cong, M., Liu, D., Liu, Y. and Du, Y. (2016), Automatic path and trajectory planning for laser cladding robot based on cad, *in* '2016 IEEE International Conference on Mechatronics and Automation (ICMA)', IEEE, pp. 1338–1343.

Zhou, C., Yang, X. and Luan, G. (2005), 'Fatigue properties of friction stir welds in Al 5083 alloy', *Scripta Materialia* **53**(10), 1187–1191.

Zimmer-Chevret, S., Jemal, N., Langlois, L., Ben Attar, A., Hatsch, J., Abba, G. and Bigot, R. (2014), FSW process tolerance according to the position and orientation of the tool: requirement for the means of production design, *in* 'Materials Science Forum', Vol. 783, Trans Tech Publ, pp. 1820–1825.

Zimmer, S., Laye, J., Langlois, L. and Bigot, R. (2008), Overview of the mean of production used for FSW., *in* 'Proc. of 7th International Friction Stir Welding Symposium', Awaji island, Japan.

Appendix A: Models matrix properties and numerical parameter values

Numerical length values of each link: $L_{1z} = 1.045\,\text{m}$, $L_{1x} = 0.500\,\text{m}$, $L_2 = 1.300\,\text{m}$, $L_{34} = 1.025\,\text{m}$, $D_4 = -0.055\,\text{m}$, $L_5 = 0.290\,\text{m}$, $L_{tz} = 0.50630\,\text{m}$.

The gearbox ratio matrix is given by $N = [N_{ij}]$. The non-null elements of N are as follow: $N_{11} = 469.375$, $N_{22} = 469.375$, $N_{33} = -504.770$, $N_{44} = -260.619$, $N_{55} = -251.977$, $N_{66} = 164.570$, $N_{54} = -1.0964$, $N_{64} = -1.5836$, $N_{65} = 1.5311$.

The coefficients of the diagonal of the stiffness matrix are: $K_1 = 6.61\,10^6$, $K_2 = 7.16\,10^6$, $K_3 = 3.08\,10^6$, $K_4 = 5.6\,10^5$, $K_5 = 6.6\,10^5$, $K_6 = 4.7\,10^6$. The units are all Nm /rd.

The relation (5) between the yaw, pitch and roll angles variation and the joint angle speed is characterized by the matrix L_a defined by:

$$L_a = \begin{bmatrix} I_3 & 0_3 \\ 0_3 & L_b \end{bmatrix} \tag{13}$$

where $L_b = \begin{bmatrix} \cos(A)\tan(B) & \sin(A)\tan(B) & 1 \\ -\sin(A) & \cos(A) & 0 \\ \cos(A)/\cos(B) & \sin(A)/\cos(B) & 0 \end{bmatrix}$ with A, B and C are the yaw, pitch and roll angles used by the controller.